Eur. Phys. J. C 6, 637–645 (1999)
DOI 10.1007/s100529800953

THE EUROPEAN PHYSICAL JOURNAL C

The hadronic contribution to the muon $g-2$ from hadron production in initial state radiation events at the e^+e^- collider DAΦNE

S. Spagnolo[a]

Dipartimento di Fisica dell'Università di Lecce and INFN, Sezione di Lecce, via Arnesano I-73100 Lecce, Italy

Received: 27 April 1998 / Published online: 26 August 1998

Abstract. A relevant reduction of the theoretical uncertainty on the muon anomalous magnetic moment, dominated by the error on the leading hadronic contribution $a_\mu^{\rm h}$, would come from a new precise measurement of the cross section of e^+e^- annihilation into hadrons (σ_h) below 1 GeV. An experimental approach to the evaluation of the dispersion integral defining $a_\mu^{\rm h}$ is proposed here as an alternative to the conventional method based on the interpolation of different measurements of σ_h performed with a center of mass energy scan. The wide occurrence of hadron production, at variable q^2, in the initial state radiation (ISR) events at the high luminosity ϕ-factory DAΦNE suggests to redefine the dispersion integral in terms of the differential cross section for $e^+e^- \to hadrons + \gamma_{\rm ISR}$. The feasibility of such measurement, which can be performed without the need of dedicated run conditions and with the benefit of the full luminosity of the machine, is discussed. The required precision is shown to be easily achieved thanks to the resolutions and performances of the KLOE detector.

1 Introduction

The E821 experiment at the AGS of BNL will measure the anomalous magnetic moment of the muon ($a_\mu = (g-2)_\mu$) with an error of the order of 0.4×10^{-9} [1], thus improving the latest result [2] by a factor of twenty.

This will increase the sensitivity to virtual effects in $(g-2)_\mu$ related to physics lying at high energy scales and, potentially, will allow to effectively constrain new physics [3], provided the Standard Model prediction [4] is affected by uncertainties of smaller or comparable size. At the moment, the most relevant theoretical error on the muon anomaly comes from the leading QCD contribution (see Fig. 1), which is calculated through the well known dispersion relation [5]

$$a_\mu^{\rm h} = \frac{1}{\pi} \int_{4m_\pi^2}^{+\infty} {\rm d}s \, \sigma_h(s) \cdot K(s). \qquad (1)$$

involving the hadronic cross section in e^+e^- collision, σ_h. The theoretical error has, therefore, an experimental origin and, in particular, is related to the poorly known cross section at low momentum transfer, which is overwhelming enhanced in the integral by the sharp increase, at $s \to 0$, of the kernel function $K(s)$, defined as follows:

$$K(s) = \frac{1}{4\pi^2} \int_0^1 {\rm d}z \frac{z^2(1-z)}{z^2 + s(1-z)/m_\mu^2}.$$

[a] Presently at Rutherford Appleton Laboratory, Chilton, Didcot, Oxfordshire OX11 0QX, UK
E-mail: Stefania.Spagnolo@rl.ac.uk

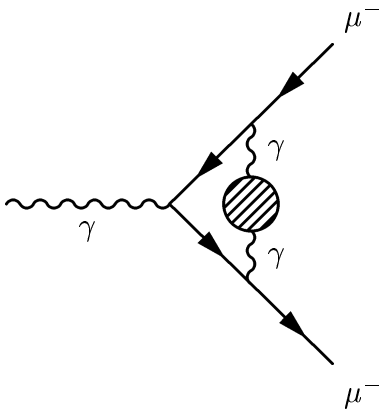

Fig. 1. The leading hadronic contribution to the muon anomalous magnetic moment originates at order α^2 from the hadronic vacuum polarization of a virtual photon exchanged between the incoming and the outcoming muon

According to the analysis in [6], where the hadronic contribution, at one loop, to the anomalous magnetic moment of the muon is estimated to be $a_\mu^{\rm h} = (70.235 \pm 0.585^{\rm stat} \pm 1.409^{\rm syst}) \cdot 10^{-9}$, the range of energies below 1.4 GeV accounts for 77% of the total quadratic error, the ρ resonance region being responsible for 62% of it.

A more recent analysis [7] has reached a 37% reduction of the error quoted in [6] by exploiting the new data from hadronic τ decays [8] that can be related to σ_h through isospin rotation, once CVC is assumed. Nevertheless, the

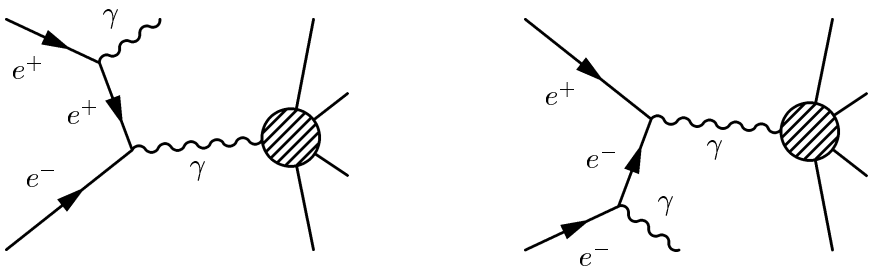

Fig. 2. Feynmann diagrams or the process $e^+e^- \to \gamma + hadrons$ where the photon is emitted from the initial state. The blob represents the color interactions leading to the hadronic final state

ρ resonance region is still responsible for more than 50% of the overall quadratic uncertainty.

The possibility that the ϕ-factory DAΦNE could provide a further improvement of the precision on $(g-2)_\mu$ has been often discussed [9]. The measurement of the hadronic cross section on a fine grid of points, in the range of s extending from threshold up to 1 GeV^2, has been shown to easily meet the goal of a precision of $0.15 \cdot 10^{-9}$ on the corresponding contribution to $a_\mu^{\rm h}$, at least from the point of view of the statistical error and of the systematics arising from the absolute energy scale and from the luminosity monitoring. Unfortunately, a scanning of the collider energy, which would require a dedicate tuning of the machine, is not envisaged at short term.

In this note we show that an alternative approach to the measurement exists, that can be exploited while DAΦNE runs at $\sqrt{s} = {\rm M}_\phi$. It consists in looking at the events in which the radiation of a photon in the initial state is followed by the annihilation of the e^+e^- pair into hadrons. The sub-process of hadron production occurs at the value of the four-momentum squared $s' = {\rm M}_\phi^2 - 2E_\gamma {\rm M}_\phi$, which varies in a continuous fashion according to the energy (E_γ) spectrum of the radiated photon. The high luminosity of DAΦNE at the design energy, $\mathcal{L}({\rm M}_\phi) = 5 \times 10^{32}$ cm^{-2}s^{-1}, allows for a sufficient statistics to be collected during the long run time devoted to the CP violation studies, in spite of the suppression α of the production rate for such events.

In the following, this hypothesis is quantitatively verified and a scheme of principle of the measurement is outlined by assuming a luminosity of DAΦNE of $3 \cdot 10^{32}$ cm^{-2} s^{-1} (a factor 3/5 less than the peak performance of the collider) and a run time of the order of one year (throughout the paper we assume 1 year=10^7 s). Moreover, the measurement is supposed to be performed in the KLOE experiment [10] and, therefore, the typical resolutions of the KLOE subdetectors [11,12], a drift chamber (DC) and an electromagnetic calorimeter (EmC), are assumed. The effect of the main source of error, which consists in the uncertainty on the photon energy, is discussed in some detail and an unfolding procedure is applied to a simulated photon spectrum.

The proposed method of measurement leads, potentially, to an interesting improvement on the present knowledge of the hadronic contribution to a_μ.

2 The method

In the process $e^+e^- \to \gamma\gamma^\star \to \gamma + hadrons$, depicted in Fig. 2, the radiation of the real photon and the hadron production can be factorized and the differential cross section is usually [13,14] written as:

$$\frac{{\rm d}\sigma}{{\rm d}E_\gamma} = 2\,\frac{\sigma_h(s')\,H(x,s,\theta_{min})}{\sqrt{s}} \tag{2}$$

In the above equation E_γ represents the energy of the real photon and s is, in our case, ${\rm M}_\phi^2$. The cross section for hadron production, σ_h, is evaluated at the rescaled four-momentum $s' = s(1-x)$, where $x = 2E_\gamma/{\rm M}_\phi$ is the fraction of the energy lost by the e^+, or e^-, in the radiation process. Since the angular distribution of the radiated photons favours small values of the angle θ between the photon flight line and the beam, the radiation function $H(x,s,\theta_{min})$ depends quite critically on the minimum angle matching the definition of the geometrical acceptance of the photon detector (see Fig. 3). The analytic expression for H is

$$H(x,s,\theta_{min}) = \frac{\alpha}{\pi}\frac{2(1-x)+x^2}{x}\left[\ln\left(\frac{1+\beta_e\cos\theta_{min}}{1-\beta_e\cos\theta_{min}}\right) - \frac{\cos\theta_{min}}{\gamma_e(1-\beta_e^2\cos^2\theta_{min})}\right]$$

where β_e and γ_e are the velocity end the relativistic factor of the electrons (and positrons) in the beam.

Equation (2) establishes a link between the cross section for the events $e^+e^- \to \gamma\gamma^\star \to \gamma + hadrons$ and the hadronic cross section σ_h that can be used in order to express in a different fashion the dispersion integral in (1). Indicated with $\mathsf{a}_\mu^{\rm h}$ the fraction of the hadronic contribution to the muon $g-2$ related to a restricted integration domain, one has:

$$\mathsf{a}_\mu^{\rm h} = \frac{1}{\pi}\int_{s_{\rm min}}^{s_{\rm max}} {\rm d}s\,\sigma_h(s)\,K(s) = \\ = \frac{{\rm M}_\phi^2}{\pi}\int_{E_{\gamma{\rm down}}}^{E_{\gamma{\rm up}}} {\rm d}E_\gamma \frac{K(s(E_\gamma))}{H(x(E_\gamma),{\rm M}_\phi^2,\theta_{min})}\,\frac{{\rm d}\sigma(E_\gamma)}{{\rm d}E_\gamma}\,. \tag{3}$$

From the experimental point of view, the computation of the integral in (3) requires the definition of a partition of the global photon energy range ($E_{\gamma{\rm up}} - E_{\gamma{\rm down}}$) into a

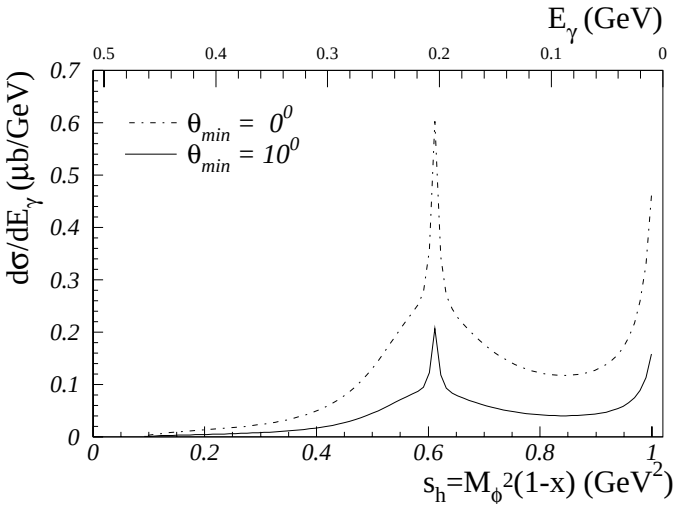

Fig. 3. Differential cross section for hard bremsstrahlung in the initial state of the process $e^+e^- \to$ *hadrons* as a function of the invariant mass of the hadron system. The corresponding scale of energy of the radiated photon is also shown

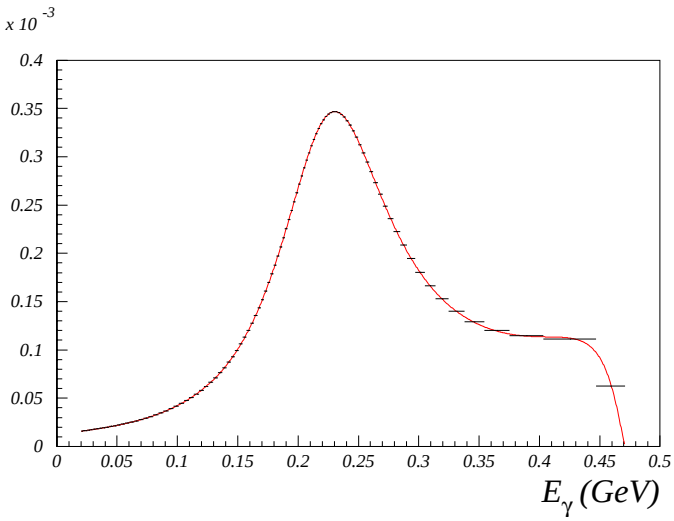

Fig. 4. The solid line represents the differential cross section multiplied by K/H; the superimposed step function is obtained by normalizing the number of events in each bin to the bin width and to the integrated luminosity and multiplying it by K/H computed at the center of the bin. No experimental resolutions have been taken into account

sequence of N bins; then the integral translates into the following finite sum:

$$\mathtt{a}_\mu^{\mathrm{h}} = \frac{\mathrm{M}_\phi^2}{\pi\,\mathcal{L}_{int}} \sum_{i=1}^{N} \frac{K_i}{H_i}\, N_i^{ev}, \qquad (4)$$

where N_i^{ev} is the number of events collected in the i$-th$ photon energy bin and $\mathcal{L}_{int}$ is the total integrated luminosity corresponding to the whole period of data taking. Equation (4) relies on the approximation that the functions K and H can be evaluated at some value of the hadron energy for each energy bin, instead of being multiplied by the differential cross section and integrated. As a consequence, a small average bin width is required.

In the following, in order to simulate the measurement, we assume a parameterization of the hadronic cross section based on a Breit-Wigner description of the ρ resonance curve and of the continuum production of pairs of charged pions. In such a way, by considering only the $\pi^+\pi^-$ final state, we overcome the problems arising from the sharp trend of σ_h at $\sqrt{s} \approx \mathrm{M}_\omega$.

The energy of the hadronic system is kinematically allowed to reach the threshold for hadron production $2m_\pi$, corresponding to $E_\gamma \simeq 471$ MeV. Therefore, the boundary of the photon energy interval are set to 20 MeV and 471 MeV. The lower bound comes from an experimental requirement, since the KLOE electromagnetic calorimeter provides a fully efficient detection (and a good energy measurement) for γ's energies greater than 20 MeV. A reasonable criterion for defining the interval partition is to keep constant the number of events in each bin, once a total number of bins $N = 100$ is assumed. This implies a typical bin width, ΔE_γ, of a few MeV slowly increasing at $s' > \mathrm{M}_\rho^2$ and leads to the approximation of the function to be integrated in (2), $(K/H)\mathrm{d}\sigma/\mathrm{d}E_\gamma$, with the step function shown in Fig. 4. The approximation error induced by the finite sum $(f.s.)$ is $\mathtt{a}_\mu^{\mathrm{h}}(f.s.) - \mathtt{a}_\mu^{\mathrm{h}}(integration) = 0.14 \cdot 10^{-9}$ and 50% of it comes from the last bin, where the cross section steeply drops as $\sqrt{s}$ approaches the threshold $2m_\pi$. In the following, we will assume as goal for the measurement an uncertainty on $\mathtt{a}_\mu^{\mathrm{h}}$ below $0.15 \cdot 10^{-9}$ and, for the seek of simplicity, we will not consider the last bin by restricting our study to the interval 20 MeV $< E_\gamma <$ 450 MeV. Lower energies of the hadron system could be accessed by splitting the last bin, since, as it will be shown, the statistical fluctuations are not a relevant limiting factor for the precision of the measurement. Finally, hereafter $\theta_{min} = 10^\circ$ will be adopted as cut-off angle for photon detection.

Table 1. The statistical error due to fluctuations in the event counting in bins of the partition

Run time (years)	$\mathtt{a}_\mu^{\mathrm{h}}(f.s.) - \mathtt{a}_\mu^{\mathrm{h}}(int)$ (10^{-9})	$\sigma(\mathtt{a}_\mu^{\mathrm{h}}(f.s.))$ (10^{-9})	N^{ev}/bin (10^5)
1/3	0.069	0.018	1.75
1/2	0.070	0.015	2.62
1	0.070	0.011	5.25
2	0.070	0.008	10.5

2.1 Statistical error and detection efficiencies

The uncertainty due to the statistical fluctuation of the number of events collected in each bin can be easily evaluated by simulating several calculations of the sum in (4), in which the number of events in each bin is randomly extracted from a poissonian distribution with average equal to the expected value. Then, the standard deviation of the distribution of the resulting estimates of $\mathtt{a}_\mu^{\mathrm{h}}$ gives the statistical error of the measurement. As shown in Table 1, the assumed luminosity ($3 \cdot 10^{32}$ cm^{-2}s^{-1}) entails a negligible statistical error, with respect to the approximation

error, also in the case of a short run time. As expected, the average of the distribution turns out to be shifted, with respect to the value of $\mathsf{a}_\mu^{\mathrm{h}}$ resulting from the integration, by the amount $0.07 \cdot 10^{-9}$.

The overall efficiency for the ISR events with a pair of charged pions in the final state is the result of the following main factors: the trigger efficiency (ϵ_{trg}), the geometrical acceptance for the photon (ϵ_g^0) and for the pair of pions (ϵ_g^{+-}), the efficiency of detection for the photon (ϵ^0) and the efficiency of detection and reconstruction of a pair of charged tracks coming from the interaction region (ϵ^{+-}).

The suppression in statistics arising from the geometrical acceptance for the photon has already been taken into account in the radiation function with the choice of the θ_{min} angle. For the sample of events satisfying the basic requirements $|\theta| > \theta_{min}$ and $E_\gamma > 20$ MeV, the trigger efficiency should be practically 100%. In such conditions, the KLOE electromagnetic calorimeter provides fully efficient photon detection and the two charged tracks are very likely to provide signals in the drift chamber or at least, in case of very small transverse momenta, in the inner part of the end-cap calorimeter. Moreover, a trigger requiring signals either in the drift chamber or in the calorimeter would surely improve the efficiency. In fact, the momentum (and therefore the average transverse momentum, which determines the number of crossed layers in the drift chamber) of the charged particles increases as the photon energy decreases (and therefore as the probability of missing a photon signal in the EmC increases). As a consequence, a low probability of photon detection corresponds to a high probability of signals in the DC from the pion tracks, and conversely.

Results on prototypes and on the EmC modules in cosmic ray stands [11] assure that ϵ^0 can be considered equal to 1 irrespective of the photon energy, provided the threshold of 20 MeV is passed.

The hardware efficiency of the KLOE DC, 99.7% in a prototype study [12,16], assures that the detection inefficiency for charged particles can be neglected with respect to the reconstruction efficiency. Therefore, a reasonable guess for ϵ^{+-} is provided by the well studied efficiency of the KLOE tracking algorithm for $\pi^+\pi^-$ pairs coming from K_S decays. Following [17], the efficiency for single track exceeds 90% and mildly depends on the number of hits and on the dip angle of the track.

The geometrical acceptance for the charged particles depends on the energy and on the direction of emission of the radiated photon. Also, the relative orientation of the particle with respect to the direction of the photon determines the transverse momentum in the laboratory frame.

A quantitative and conservative, although not refined, estimate of the overall efficiency for the charged sector of the event can be obtained by assuming that the reconstruction efficiency for a single track coming from the origin is of the order of 80% provided it crosses the twelve innermost layers of the DC and so producing at least twelve hits. Then, for a given photon energy, the average geometrical efficiency is computed by counting the number of

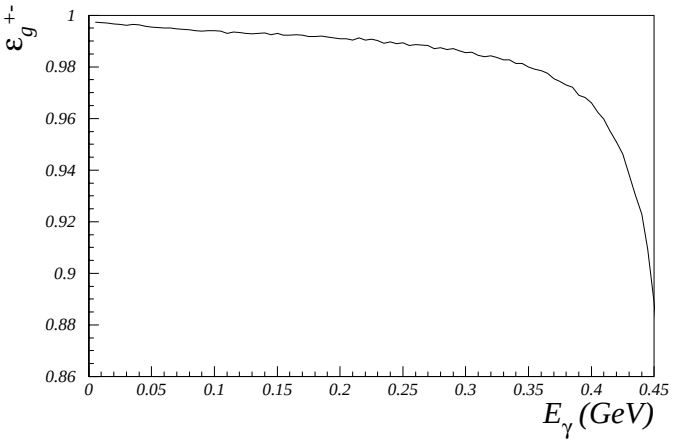

Fig. 5. Geometrical acceptance for the reconstruction of the $\pi^+\pi^-$ pair in $e^+e^- \to \gamma\pi^+\pi^-$. An event is defined reconstructable with efficiency (of reconstruction) of $\sim 65\%$ when both pions have $p_t > 45$ MeV

events in which the transverse momentum of each pion is larger than the value of 45 MeV, which correspond to the threshold for crossing the twelve layers at the core of the DC. This exercise has been performed by averaging over

- the θ angle of the photon, by taking into account the proper angular distribution,
- the angle of emission of the pions in their center of mass, by assuming the angular distribution ($\mathrm{d}\sigma/\mathrm{d}\Omega \propto \sin^2\theta$) for the production of a pair of pseudoscalar in e^+e^- collision [18],
- the azimuthal angle of the pion momentum, which is flat in the center of mass of the hadronic system.

The result, shown in Fig. 5, when combined with an estimate of $\epsilon^{+-} \simeq 65\%$, guarantees no critical drop in the statistics due to the overall efficiency for the charged pion reconstruction.

2.2 Angular resolution

Another source of error in the evaluation of (4) comes from the experimental uncertainty on the angular cut applied to the radiated photons. The resolution of the measurement of the photon polar angle $\delta\theta$ results into an error affecting the function H in every energy bin

$$\delta H_i = \frac{\partial H}{\partial \theta_{min}} \delta\theta_{min}$$

where $\delta\theta_{min}$ is given by the measurement error scaled by the square root of the number of events contributing to the statistical definition of the boundary of the acceptance region. An uncertainty $\delta\theta_{min} < 1$ mrad assures that the corresponding error on a_μ is smaller than $2 \cdot 10^{-11}$ and, therefore, negligible. This goal can be easily achieved thanks to the DC angular resolution that, also in case of low momenta of the two pions (i.e. few hits per track and large contribution to the error in the track reconstruction from multiple Coulomb scattering) allows to reach single

track resolutions of the order of $\delta\theta = 10$ mrad. Hence, the large statistics collected in each energy bin allows to define the edge of the acceptance region much better than 1 mrad.

On the other hand, systematic errors in the measurement of the photon polar angle would be smaller than 0.1 mrad, due to the relative alignement of the KLOE subdetectors that will be controlled within ~ 100 μm. Moreover, eventual asymmetries in the yields of very aboundant processes, like Bhabha scattering, will provide a constant monitor of the proper definition of the global reference frame. As a consequence, no relevant systematic errors can arise in the overall normalization.

2.3 Energy resolution

A more relevant effect on the evaluation of $\mathsf{a}_\mu^{\rm h}$ is produced by the resolution on the energy scale. The direct measurement of the energy of the radiated photons would be provided by the electromagnetic calorimeter of KLOE, which in fact exhibits excellent energy resolution [11], with an error parameterized by the relation

$$\frac{\sigma(E_\gamma)}{E_\gamma} = \frac{5\%}{\sqrt{E_\gamma(\mathrm{GeV})}} \qquad (5)$$

where constant systematic terms are irrelevant. Therefore, by denoting with E^m the measured energy of the photon, the actual spectrum of the photons in the ISR events, for which the energy measurement falls in the i-th bin, is:

$$\frac{\mathrm{d}N(E_\gamma)}{\mathrm{d}E_\gamma} \propto \frac{\mathrm{d}\sigma(\mathrm{E}_\gamma)}{\mathrm{d}E_\gamma} \int_{\Delta E_i} \mathrm{d}E^m g(E^m, E_\gamma), \qquad (6)$$

where $g(E^m, E_\gamma)$ is the value of a gaussian, of average E_γ and sigma given by (5), computed at E^m. For a bin of width $\Delta E_i = 2$ MeV with center at $E_\gamma = 200$ MeV the FWHM of the photon spectrum is approximately 50 MeV. Since the differential cross section is not constant, the migration of events from one bin to the neighboring ones, induced by the finite resolution, produces a large distortion of the global distribution of events (see Fig. 6).

The resulting systematic error on the evaluation of $\mathsf{a}_\mu^{\rm h}$ is

$$\delta\mathsf{a}_\mu^{\rm h} = \mathsf{a}_\mu^{\rm h}(E_\gamma res) - \mathsf{a}_\mu^{\rm h}(integration) = 0.17 \cdot 10^{-9}.$$

One has to point out that, in spite of the quite large distortion of the energy spectrum, the overall effect on the sum is small, although it exceeds the imposed limit. This occurs as a benefit of the integral character of the measurement. Moreover, the energy resolution so far considered is a pessimistic estimate of what is going to happen in the real experiment. In fact, the excellent momentum resolution of the KLOE detector allows to measure very accurately the momentum of the charged pions and the fluctuations of the photon energy measurement can be strongly reduced by imposing energy and momentum conservation in the event.

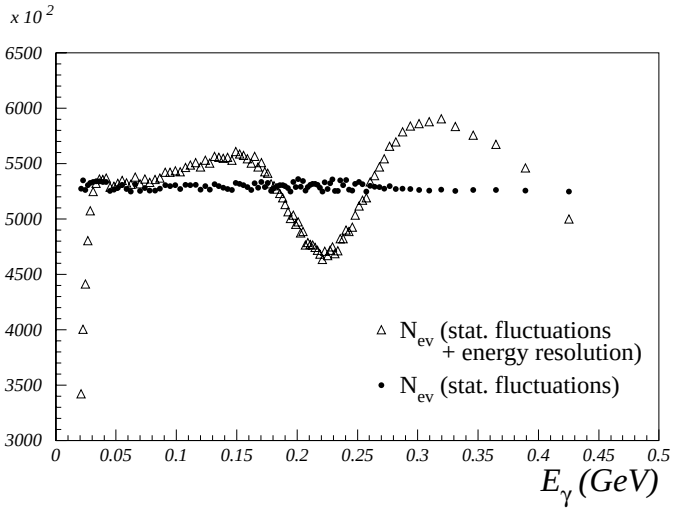

Fig. 6. Number of yields in each bin (as a function of the central value of the photon energy in the bin) for an ideal energy resolution compared to the number of events observed as a consequence of the resolution in (5). In both cases the statistical fluctuations have been simulated

Nevertheless, in the next section we will show that the application of a standard deconvolution procedure to the observed γ spectrum can correct for the distortion in Fig. 6 thus pushing down the error below the acceptable threshold, also in case of a direct determination of the photon energy.

3 Deconvolution of the energy resolution

Several techniques have been developed for the treatment of measured data affected by experimental resolutions. A very general and powerful approach to the deconvolution problem [19] is based on the Bayes theorem.

In the statistical process under consideration, one can distinguish N_E effects, which are the 99 bins of measured energy E_j^m, and $N_C = 101$ causes to be identified with the same intervals of "real" photon energy plus the two bins $0 < E_\gamma < 20$ MeV and 450 MeV $< E_\gamma <$ 471 MeV. The actual population of the i$-th$ energy bin ($\tilde{n}(E_{\gamma_i})$) can be inferred from the measured distribution ($n(E_j^m)$) through the relation

$$\tilde{n}(E_{\gamma_i}) = \frac{1}{\epsilon_i} \sum_{j=1}^{N_E} n(E_j^m) P(E_{\gamma\, i} \mid E_j^m) \; ;$$
$$\epsilon_i = \sum_{j=1}^{N_E} P(E_j^m \mid E_{\gamma_i}) \qquad (7)$$

The knowledge of the detector response allows to know the conditional probability of the effects $P(E_j^m|E_{\gamma_i})$ and the Bayes theorem

$$P(E_{\gamma_i} \mid E_j^m) = \frac{P(E_j^m \mid E_{\gamma_i}) P(E_{\gamma_i})}{\sum_{k=1}^{N_C} P(E_j^m \mid E_{\gamma_k}) P(E_{\gamma_k})}$$

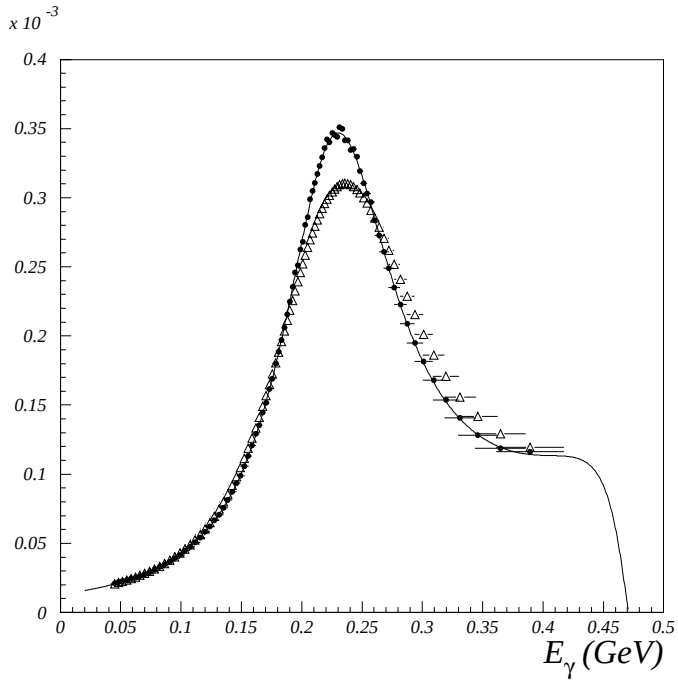

Fig. 7. Distribution of the ISR photon energy multiplied by $K/(H\mathcal{L}_{int})$. The solid line is the ideal distribution, the effect of energy resolution and statistical errors is represented by the triangles. The deconvolution technique nicely recovers the original shape of the distribution (full dots)

relates it to the conditional probability of the causes (needed for the evaluation of (7)) and to the probability distribution of the causes ($P(E_{\gamma_i})$). A rough initial estimate of $P(E_{\gamma_i})$ allows to apply iteratively (7) by updating, at every new step, the estimate of $P(E_{\gamma_i})$ with the previously determined $\tilde{n}(E_{\gamma_i})$ normalized to the total number of events.

This procedure has been applied to the simulated measured distribution in Fig. 6 by evaluating the conditional probability of the effects according to the calorimeter resolution

$$P(E_j^m \mid E_{\gamma_i}) = \int_{\Delta_i} \mathrm{d}E_\gamma \int_{\Delta_j} \mathrm{d}E^m \, \frac{1}{\sqrt{2\pi}\sigma(E_\gamma)} \, e^{-\frac{(E^m - E_\gamma)^2}{2\sigma^2(E_\gamma)}}.$$

The result is shown in Fig. 7 for a restricted energy region since the deconvolution procedure produces, as a natural drawback, artificial oscillations at the boundary of the distribution. Optimizations of the method, based on a smoothing of the spectrum at each iteration, are well established [19] and assure that a proper cure of this artefact can be implemented, thus recovering the boundary regions of the integration domain.

After the deconvolution, the calculation of $\mathsf{a}_\mu^{\mathrm{h}}$ according to (4) in the range 28 MeV $< E_\gamma <$ 403 MeV (which corresponds to the range of invariant mass for the $\pi^+\pi^-$ pair 0.218 GeV$^2 \div$ 0.984 GeV^2), is affected by the error

$$\delta\mathsf{a}_\mu^{\mathrm{h}} = \mathsf{a}_\mu^{\mathrm{h}}(\mathit{full\ simulation}) - \mathsf{a}_\mu^{\mathrm{h}}(\mathit{integration}) = 0.094 \cdot 10^{-9}.$$

The statistical and systematic contributions to the error are

$$\delta\mathsf{a}_\mu^{\mathrm{h}\,stat} = 1.7 \cdot 10^{-11}\ ; \quad \delta\mathsf{a}_\mu^{\mathrm{h}\,sist} = 9.2 \cdot 10^{-11}\ .$$

where, the former comes from the hypothesis of 1 year of run (10^7 s at $\mathcal{L} = 3 \cdot 10^{32}$ cm^{-2}s^{-1}) and efficiencies as described above (a part from a very pessimistic 10% inefficiency assumed for the photon detection) and the latter is the result of the approximation of the the integral with a finite sum and of the energy resolution of the EmC.

One should stress that a three times lower luminosity of the collider would lead to an increase of the statistical error by no more than a factor of two, as shown in Table 1, thus keeping unchanged the dominance of the systematic uncertainty.

4 Backgrounds

It is useful to distinguish among the backgrounds for the events so far considered those with the same final state of the signal and those with final state that can simulate $\pi^+\pi^-\gamma$.

To the latter kind belongs the process $e^+e^- \to \mu^+\mu^-\gamma$, where the photon comes from ISR, which occurs with a rate ~ 2.6 times smaller than the signal events (by averaging over the γ energy). Moreover, the very good momentum resolution of the KLOE drift chamber allows to reach a resolution on the total energy in the event of a few MeV. A conservative estimate of 5 MeV gives a signal over background ratio $\mathcal{S}/\mathcal{B} = 54$, if one selects the signal by requiring that the total energy, computed as $E_+ + E_- + |\mathbf{p}_+ + \mathbf{p}_-|$ (where $E_\pm = \sqrt{|\mathbf{p}_\pm|^2 + m_\pi^2}$ is the energy associated to the charged particles), differs from M_ϕ by less than 8 MeV. Moreover, since the cross section for this background process is very well known, its subtraction introduces a negligible systematic error.

Further sources of background, which simulate the signal topology if one photon escapes the detection, are

- $\phi \to 3\pi$ (which proceeds in 83% of the cases through a $\rho\pi$ intermediate state) with a cross section of 0.67 μb;
- $\phi \to \eta\gamma$ (BR=1.26%) with $\eta \to \pi^+\pi^-\gamma$ (BR= 4.78%).

In both cases the dangerous situation consists in the presence of a photon of energy lower than 20 MeV (especially if such a photon falls into the cone of 10° not seen by the EmC) while the second γ is inside the acceptance region. In the 3π final state the spectrum of the second photon is continuous while in the $\eta\gamma$ radiative decay of the ϕ the narrow width of the η entails $E_\gamma = 363$ MeV and allows to easily identify and statistically isolate the background. Moreover in the last case, the expected number of events is $\sim 1/100$ of the total signal rate and, therefore the $\mathcal{S}/\mathcal{B}$ in the energy bins around $E_\gamma = 363$ MeV would be of order (but larger than) 1. In the 3π case, a cut of $P(\chi^2) < 5\%$ after a kinematical fit of the event, based on momentum and energy conservation, throws away $\sim 50\%$ of such fake signal events, if the resolutions on the charged tracks can

be disregarded compared to the energy resolution and position resolution of the photon seen by the EmC. The overall (integrated over the photon energy) $\mathcal{S}/\mathcal{B}$ ratio is 2.02 for $\rho\pi$ and 10.7 for direct 3π production in the ϕ decay (we neglect the direct hadron production of three pions in e^+e^- collision since we sit on top of the ϕ resonance). The amount of background is, hence, quite small and does not constitute a dangerous source of statistical error. More critical is the systematic error arising in the background subtraction from the uncertainty on the BRs for the background processes. In particular, the spectrum of the photons in the background events surviving the cut sets in for $E_\gamma > 230$ MeV. This energy interval accounts for more than 50% of $\mathtt{a}_\mu^{\mathrm{h}}$, therefore, the present relative error on BR($\phi \to \rho\pi$), which is $\varepsilon \simeq 5.4\%$ [20], entails a relative error on the corresponding integral ($\sim \mathtt{a}_\mu^{\mathrm{h}}/2$) of order $\varepsilon/(\mathcal{S}/\mathcal{B}) \approx 2.5\%$ for $\mathcal{S}/\mathcal{B} = 2$ (in fact the number of signal events is evaluated as

$$N - N/(1+\mathcal{S}/\mathcal{B}) \pm \varepsilon \times N/(1+\mathcal{S}/\mathcal{B})$$

where N is the total number of yields, signal plus background). This error means an absolute uncertainty on $\mathtt{a}_\mu^{\mathrm{h}}$ exceeding $0.6\cdot10^{-9}$ well above the required precision. Nevertheless, the huge sample of $\phi \to 3\pi$ events produced at DAΦNE will provide a new measurement of the corresponding BR with the permille precision needed in order to meet our goal.

The most abundant process leading to the final state $\pi^+\pi^-\gamma$ at DAΦNE is the ISR followed by hadron production in the annihilation of e^+e^-. Nevertheless, several other processes contributing to the same final state exist; they are

A_1) the ϕ decay into $\pi^\pm\rho^\mp$ followed by $\rho^\mp \to \pi^\mp\gamma$ (BR($\rho^\mp \to \pi^\mp\gamma) = 4.5\cdot10^{-4}$);

A_2) the final state radiation (FSR): the process is usually described by means of a coupling $\gamma \to \rho$ and then $\rho \to \pi^+\pi^-$ with one of the pions radiating a photon or $\rho \to \pi^+\pi^-\gamma$ (BR($\rho^0 \to \pi^+\pi^-\gamma) = 9.9\cdot10^{-3}$);

A_3) the radiative decay of the ϕ meson into $f_0\gamma$ with the decay of f_0 into a pair of charged pions.

The background A_1, integrated over the θ_γ angle, is suppressed with respect to the signal (for $|\theta| < 10^\circ$) by a factor 1/430 (according to [20]) so it can be safely neglected. The differential cross section for FSR events [13], integrated over the whole solid angle[1], is shown in Fig. 8 together with the ISR differential cross section in the case $\theta_{min} = 10^\circ$. In average, the signal over background ratio is $\mathcal{S}/\mathcal{B} = 17$, and the integral ratio is more than 9. Moreover in these background events the angle between the photon and the pion momentum in the dipion rest frame is small, so the $\mathcal{S}/\mathcal{B}$ ratio can be improved by a proper cut on $\theta_{\pi\gamma}$.

The most tedious feature of the background of type A is the not yet measured BR for the radiative decay

[1] In the comparison with the ISR cross section for $\theta_{min} = 10^\circ$ this is a slightly pessimistic approximation, since the angular distribution of the FSR events smoothly decreases at $|\cos(\theta)| > 0.8$

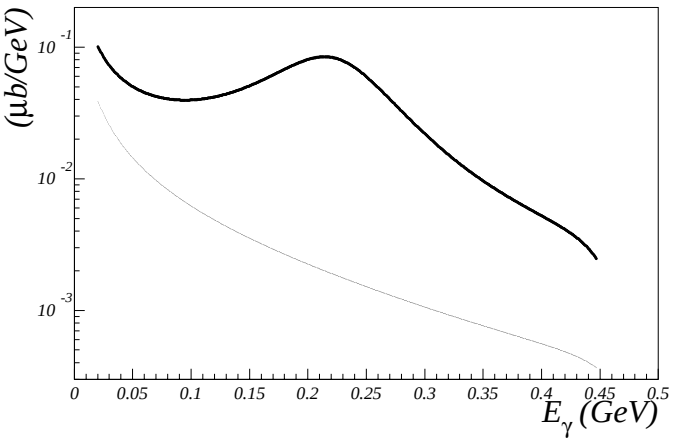

Fig. 8. Differential cross section for hard bremsstrahlung in the initial state of the process $e^+e^- \to$ *hadrons* for $\theta_{min} = 10^\circ$ (upper curve) and for final state radiation integrated over the whole solid angle (lower curve)

$\phi \to f_0\gamma$ as well as the poorly known parameters of the lightest scalar resonance f_0. The various hypothesis under debate concerning the nature of f_0 [21] lead to quite different predictions for the $BR(\phi \to f_0\gamma)$, $\mathcal{O}(10^{-4}) - \mathcal{O}(10^{-6})$, all below the present experimental limit, $7\cdot10^{-4}$ [22]. Moreover, the amplitude for the process indicated by A_3 interferes with the amplitude of A_2, since in both cases the pion pair is in a C even state, while the opposite happens in the background events of type A_1 and in the signal. According to [13], the rate for the processes A_2 and A_3 and for the interference term can be parameterized in terms of G_s, the coupling $\phi\gamma f_0$, and of g_s, the coupling $f_0\pi^+\pi^-$. Their product (absolute value and sign, which determines the kind of interference) could, in principle, be measured from the differential cross section and from the total cross section for $e^+e^- \to \pi^+\pi^-\gamma$ as a function of the total energy in the e^+e^- rest frame, as pointed out in [15]. In any case, the signal from A_3 and from the interference $A_3 - A_2$ represent a small background for the ISR events, that could be relevant, depending on the nature of the scalar meson, only for $E_\gamma < 100$ MeV. A further way out comes from the other final state accessible for $f_0\gamma$, i.e. $\pi^0\pi^0\gamma$ which does not interfere with other processes and allows to study the line shape of the scalar meson under different experimental conditions.

One should also stress that the signal over background ratio can be strongly enhanced for any of the channels discussed by releasing the cut on the angular acceptance for the radiated photon and relying on the energy and momentum conservation for the events in which the photon is not detected. This solution would require a much better estimate of the radiative corrections since the appearence of two charged pions could be related to a single hard bremstrahlung process as well as to multiple soft photon emissions.

5 Conclusions

The initial state radiation events at DAΦNE provide a copious source of events $e^+e^- \to \pi^+\pi^-$ at momentum transfer continuously varying between M_ϕ and threshold. The high luminosity of the collider and the good overall efficiency of the KLOE detector, make the sample of events suitable, from the statistical point of view, for a precise calculation of the hadronic contribution to the muon anomaly from $\sqrt{s} < M_\phi$ from the $\pi^+\pi^-$ final state. In such a way, a negligible contribution to the error affecting a_μ would arise from the ρ resonance region, thus leading to a reduction of 38% of the total uncertainty for the hadronic dominant correction as quoted in [6]. The main source of error is systematic and is related to the definition of the energy scale. The use of standard deconvolution techniques has been shown to correct for the experimental resolution effects also in the most pessimistic hypothesis of a calorimetric measurement of the energy of the radiated photon.

Some care would be required in the handling of the background subtraction. Although the ISR events are the most abundant origin of the $\pi^+\pi^-\gamma$ final state at DAΦNE, the high precision required in the measurement imposes a good control of the remnant background and also a good theoretical description of the processes concurring to the same final state.

Moreover, the achievement of a significant improvement in the calculation of $\mathsf{a}_\mu^{\rm h}$ requires a low experimental error on the global normalization, i.e. the luminosity measurement, and a high accuracy of the theoretical evaluation of all the relevant radiative corrections to the differential cross section. While luminosity can be easily controlled by monitoring the large angle Bhabha scattering, as already discussed in [9], the theoretical accuracy could become the limiting factor for the accuracy on $\mathsf{a}_\mu^{\rm h}$, since a precision on the radiator H of the order of a few permille is needed in order to keep the overall error at the level of $1.5 \cdot 10^{-10}$.

The present study, without aiming at providing a full outline of the measurement, shows that no inherent experimental limits forbid to pursue an experimental approach to the evaluation of the hadronic leading contribution alternative to the energy scanning. Indeed room is left for the optimization of many steps of the study, in particular the energy binning with respect to the possibility of enlarging the integration interval and of minimizing the statistical and systematic error. Some general benefits of the integral character of the measurement, compared to the discrete scanning of the energy interval, have also been pointed out during the discussion.

Of course, the ultimate accuracy of the measurement can be evaluated only with a full simulation of the data and of the detector response, but the application of this measurement method at DAΦNE seems to promise a relevant reduction of the error on $a_\mu^{\rm h}$ from an energy region in which no other possibilities of measuring σ_h are in sight in the next future. Moreover, the general method allows to explore energy intervals otherwise unaccessible by the present and future e^+e^- colliders. For example, the theoretical prediction on $\Delta\alpha_{em}(M_Z^2)$, whose hadronic contribution is calculated with a dispersion integral of σ_h and suffers from the lack of precision in the data of e^+e^- collision below 10 GeV, could probably benefit of the bulk of ISR events produced at the forthcoming collider PEP-II, running at $\sqrt{s} = M_\Upsilon$.

Acknowledgements. The author is indebted to prof. G. Pancheri for the useful discussions and suggestions which stimulated the present study. She thanks also prof. C. Verzegnassi for introducing her to the subject of the anomalous magnetic moment of the muon and dr. F. Grancagnolo for having followed the analysis of the experimental errors affecting the measurement.

References

1. V.W. Hughes et al., "The anomalous magnetic moment of the muon" Bonn 1990, Proceedings, High energy spin physics, vol. 1, 367–382; B.L. Roberts, "The new muon (g-2) experiment at Brookhaven", Heidelberg 1991, Proceedings, The future of muon physics 101–108, Z. Phys. C **56**, Suppl. 101–108 (1992); E821 Collaboration (B.L. Roberts et al.) "Status of the new muon (g-2) experiment",in the proceedings of 28th International Conference on High-energy Physics (ICHEP'96), Warsaw, Poland, 25–31 Jul 1996, River Edge, NJ, World Scientific, 1997, pp. 1035
2. J. Bailey et al. Nucl. Phys. B **150**, 1 (1979)
3. for an extensive discussion of the new physics effects in the muon $g-2$ P. Méry, S.E. Moubarik, M. Perrottet, F.M. Renard, Z. Phys. C **46**, 229 (1990) and T. Kinoshita, W.J. Marciano in "Quantum Electrodynamics", ed. T. Kinoshita, World Scientific, Singapore, 1990, pp.419; some updated results can be found in G. Couture, H. Konig, Phys.Rev. D **53**, 555 (1996); T. Moroi, Phys. Rev. **D 53**, 6565 (1996); M. Carena, G.F. Giudice, C.E.M Wagner, Phys. Lett. B **390**, 234 (1997); F.M. Renard, S. Spagnolo, C. Verzegnassi, Phys. Lett. B **409**, 398 (1997)
4. The present status of the Standard Model contributions to the muon $g-2$ is overviewed in many recent papers related to the subject; the latest results are S. Laporta, E. Remiddi, Phys. Lett. B **379**, 283 (1996); B. Krause, Phys.Lett. B **390**, 392 (1997); M. Hagiwara, T. Kinoshita, A.I. Sanda, Phys. Rev. D **54**, 3137 (1996); J. Bijnens, E. Pallante, J. Prades, Nucl. Phys. B **474**, 379 (1996); A. Czarnecki, B. Krause, W. Marciano, Phys. Rev. **D 52**, 2619 (1995)
5. N. Cabibbo, R. Gatto, Phys. Rev. **124**, 1577 (1961)
6. S. Eidelman, F. Jegerlehner, Z. Phys. C **67**, 585 (1995)
7. R. Alemany, M. Davier, A. Höcker, Eur. Phys. J. C **2**, 123 (1998), LAL-97-02
8. The ALEPH Collaboration (R. Barate et al.), Z. Phys. C **74**, 387 (1997); CERN-PPE/97-013 (1997)
9. P. Franzini, "The muon gyromagnetic ratio and R_h at DAΦNE", The Second DAΦNE Physics Handbook, INFN-LNF (1995), Ed.s L. Maiani, G. Pancheri, N. Paver, vol. 2, 471; P. Franzini, "R measurement at KLOE", G. Cabibbo, "Luminosity and energy measurements at DAΦNE", contributions to the Workshop "Hadron production cross sections at DAΦNE", Karlsruhe Nov.1-2 1996

10. The KLOE Collaboration, "KLOE, a general purpose detector for DAΦNE", LNF-92/019 (IR) (1992)
11. A. Antonelli et al., Nucl. Phys. B (Proc. Suppl.) **54B**, 14 (1997); G. Lanfranchi for the KLOE Calorimeter Group, "The KLOE ElectroMagnetic Calorimeter", contribution to International Conference on Calorimetry in HEP, Tucson, USA, Nov. 1997
12. A. Andryakov et al., Nucl. Inst. and. Meth. **A 404**, 248 (1998)
13. A. Bramon, G. Colangelo, P.J. Franzini, M. Greco, "$\phi \to \pi^+\pi^-\gamma$ at DAΦNE" and P.J. Franzini, W. Kim, J. Lee-Franzini, "Studying the f_0 and η' at DAΦNE", The DAΦNE Physics Handbook, INFN-LNF (1994), Ed. L. Maiani, G. Pancheri, N. Paver, vol. 2, 487; A. Bramon, M. Greco, "Scalar mesons and $\phi \to \pi\pi\gamma$ at DAΦNE", The Second DAΦNE Physics Handbook, INFN-LNF (1995), Ed. L. Maiani, G. Pancheri, N. Paver, vol. 2, 663
14. Many theoretical studies of single photon emission in the initial state at e^+e^- colliders exist in the literature; some example are G. Bonneau, F. Martin, Nucl. Phys. B **27**, 381 (1971); M. Greco, Riv. Nuovo Cim. **11**, N.5 (1988); O. Nicrosini, L. Trentadue, Nucl. Phys. B **318**, 1 (1989)
15. N.N. Achasov, V.V. Gubin, E.P. Solodov, Phys. Rev. D **55**, 2672 (1997)
16. A. Andryakov et al, "Results from the full length prototype of the KLOE drift chamber", presented at VII Pisa Meeting on Advanced Detector, Elba, May 1997; to appear in Nucl. Instr. and Meth. A
17. A. Andryakov, "Analysis of charged track reconstruction in production of 10^6 events", KLOE memo n.55 (1996) (unpublished)
18. A. Bramon, M. Greco, "Electromagnetic form factors", The Second DAΦNE Physics Handbook, INFN-LNF (1995), Ed. L. Maiani, G. Pancheri, N. Paver, vol. 2, 451
19. G. D'Agostini, Nucl. Inst. and Meth. A **362**, 487 (1995)
20. Particle Data Group, Phys. Rev. D **54**, 1 (1996)
21. F. Close, N. Isgur, S. Kumano, Nucl. Phys. B **389**, 513 (1993); R.L. Jaffe, Phys. Rev. D **19**, 267 (1977)
22. CMD-2 Collaboration (R.R. Akhmetshin et al.), Phys. Lett. B **415**, 452 (1997)